

RESEARCH BRIEF

Dominant Role of Oncogene Dosage and Absence of Tumor Suppressor Activity in *Nras*-Driven Hematopoietic Transformation

Jin Xu¹, Kevin M. Haigis³, Ari J. Firestone¹, Megan E. McNerney⁵, Qing Li⁸, Elizabeth Davis⁶, Shann-Ching Chen⁹, Joy Nakitandwe⁹, James Downing⁹, Tyler Jacks⁴, Michelle M. Le Beau⁷, and Kevin Shannon^{1,2}

ABSTRACT

Biochemical properties of Ras oncoproteins and their transforming ability strongly support a dominant mechanism of action in tumorigenesis. However, genetic studies unexpectedly suggested that wild-type (WT) *Ras* exerts tumor suppressor activity. Expressing oncogenic *Nras*^{G12D} in the hematopoietic compartment of mice induces an aggressive myeloproliferative neoplasm that is exacerbated in homozygous mutant animals. Here, we show that increased *Nras*^{G12D} gene dosage, but not inactivation of WT *Nras*, underlies the aggressive *in vivo* behavior of *Nras*^{G12D/G12D} hematopoietic cells. Modulating *Nras*^{G12D} dosage had discrete effects on myeloid progenitor growth, signal transduction, and sensitivity to MAP-ERK kinase (MEK) inhibition. Furthermore, enforced WT N-Ras expression neither suppressed the growth of *Nras*-mutant cells nor inhibited myeloid transformation by exogenous *Nras*^{G12D}. Importantly, *NRAS* expression increased in human cancer cell lines with *NRAS* mutations. These data have therapeutic implications and support reconsidering the proposed tumor suppressor activity of WT *Ras* in other cancers.

SIGNIFICANCE: Understanding the mechanisms of *Ras*-induced transformation and adaptive cellular responses is fundamental. The observation that oncogenic *Nras* lacks tumor suppressor activity, whereas increased dosage strongly modulates cell growth and alters sensitivity to MEK inhibition, suggests new therapeutic opportunities in cancer. *Cancer Discov*; 3(9): 993-1001. ©2013 AACR.

INTRODUCTION

RAS genes encode ubiquitously expressed proteins (N-Ras, H-Ras, K-Ras4A, and K-Ras4B) that cycle between active GTP-bound and inactive GDP-bound conformations (Ras-GTP

and Ras-GDP; ref. 1). Ras-GTP levels are regulated by the competing activities of guanine nucleotide exchange factors and GTPase-activating proteins (GAP), which enhance intrinsic Ras GTPase activity. Proteins encoded by *RAS* oncogenes, which accumulate in the GTP-bound state due to defective

Authors' Affiliations: ¹Department of Pediatrics and ²Helen Diller Family Comprehensive Cancer Center, University of California, San Francisco, California; ³Molecular Pathology Unit and Center for Cancer Research, Massachusetts General Hospital, Charlestown, ⁴Department of Biology, David H. Koch Institute for Integrative Cancer Research and Howard Hughes Medical Institute, Massachusetts Institute of Technology, Cambridge, Massachusetts; ⁵Department of Pathology, Institute for Genomics and Systems Biology, ⁶Ben May Department for Cancer Research, ⁷Section of Hematology/Oncology and Comprehensive Cancer Center, University of Chicago, Chicago, Illinois; ⁸Department of Medicine, Division of Hematology/Oncology, University of Michigan, Ann Arbor, Michigan;

and ⁹Department of Pathology, St. Jude Children's Research Hospital, Memphis, Tennessee

Note: Supplementary data for this article are available at Cancer Discovery Online (<http://cancerdiscovery.aacrjournals.org/>).

Corresponding Author: Kevin Shannon, 1450 Third Street, Room HD-240, San Francisco, CA 94158. Phone: 415-476-7932; Fax: 415-502-5127; E-mail: shannonk@peds.ucsf.edu

doi: 10.1158/2159-8290.CD-13-0096

©2013 American Association for Cancer Research.

RESEARCH BRIEF

Xu et al.

intrinsic GTP hydrolysis and resistance to GAPs, are exceedingly difficult targets for anticancer drug discovery due to their structural and biochemical properties (1).

Despite compelling evidence that oncogenic Ras proteins have dominant gain-of-function actions in cellular transformation, genetic studies in mice surprisingly have suggested that wild-type (WT) *Ras* exerts tumor suppressor activity in some cancers with oncogenic *Ras* mutations (2–5). However, mechanistic data regarding how normal Ras might antagonize oncogenic signaling are lacking.

Endogenous expression of *Nras*^{G12D} induces a myeloproliferative neoplasm in *Mx1-Cre;Nras*^{G12D/+} mice that faithfully models human chronic and juvenile myelomonocytic leukemia (CMML and JMML; refs. 4, 6, 7). Hematologic disease is greatly accelerated in homozygous *Nras*^{G12D}-mutant mice (*Mx1-Cre;Nras*^{G12D/G12D}; refs. 8, 9). We deployed a conditional *Nras*-mutant allele to assess the relative contributions of *Nras*^{G12D} oncogene dosage and tumor suppression by WT *Nras* in myeloid transformation. We find that elevated *Nras*^{G12D} expression drives myeloid transformation *in vivo* and strongly modulates cell growth, Ras signaling, and response to a targeted inhibitor *in vitro*. Consistent with these data, somatic uniparental disomy underlies loss of the WT allele in primary acute myeloid leukemia (AML) cells with *Nras*^{G12D} mutations, resulting in normal-to-increased *Nras* expression. Finally, *NRAS* expression is significantly elevated in human cancer cell lines with *NRAS* mutations, whereas *KRAS* expression is reduced, with a reciprocal pattern seen in cell lines with *KRAS* mutations.

RESULTS

We generated a Cre-dependent conditional *Nras* allele (*Nras*^{2lox2}) and conducted intercrosses to produce hemizygous (*Mx1-Cre;LSL-Nras*^{G12D/2lox2}), heterozygous (*Mx1-Cre;LSL-Nras*^{G12D/+}), and homozygous (*Mx1-Cre;LSL-Nras*^{G12D/G12D}) littermates on a C57Bl/6 strain background (Supplementary Fig. S1A). Use of this conditional *Nras*^{2lox2} allele avoids potential confounding consequences of eliminating WT *Nras* expression throughout development and allowed us to simultaneously activate *Nras*^{G12D} expression and inactivate WT *Nras* in the hematopoietic compartment after birth (4). Efficient recombination of both conditional *Nras* alleles with loss of expression was observed 2 weeks later (Supplementary Fig. S1B and S1C). Western blot analysis confirmed that N-Ras protein levels are reduced in the bone marrow of hemizygous *Nras*-mutant mice (Fig. 1A), which we hereafter refer to as *Nras*^{G12D/-}.

Consistent with recent reports (8, 9), approximately 20% of *Mx1-Cre;Nras*^{G12D/G12D} mice died prematurely from T lineage acute lymphoblastic leukemia (Supplementary Fig. S2A). Surviving animals of all three *Nras* genotypes were euthanized at 6 months of age. All *Nras*^{G12D/G12D} mice had overt myeloproliferative neoplasm, which was characterized by leukocytosis with elevated blood neutrophil counts, splenomegaly, and anemia (Fig. 1B and Supplementary Fig. S2B). In contrast, hematologic parameters were normal in age-matched *Mx1-Cre;Nras*^{G12D/+} and *Mx1-Cre;Nras*^{G12D/-} mice (Fig. 1B and Supplementary Fig. S2B). Flow cytometric analysis revealed increased numbers of immature monocytic (Mac-1⁺, Gr-1^{lo}) cells in the hematopoietic tissues of *Nras*^{G12D/G12D} mice, which is also observed in *Nf1*- and *Kras*-mutant mice with

myeloproliferative neoplasm (ref. 7; Fig. 1C). This population was not expanded in hemizygous or heterozygous *Nras*-mutant mice.

We grew colony-forming unit granulocyte macrophage (CFU-GM) progenitors to assess the cell-intrinsic effects of *Nras*^{G12D} gene dosage and the consequences of inactivating WT *Nras*. Somatic *NRAS* mutations are highly prevalent in JMML and CMML, and CFU-GM progenitors from patients with these aggressive cancers are hypersensitive to granulocyte macrophage colony-stimulating factor (GM-CSF; ref. 7). Similarly, *Nras*^{G12D/G12D} bone marrow cells show cytokine-independent CFU-GM growth and pronounced GM-CSF hypersensitivity (Fig. 1D; refs. 8, 9). In striking contrast, CFU-GM from *Mx1-Cre;Nras*^{G12D/-} and *Mx1-Cre;Nras*^{G12D/+} mice displayed normal cytokine responses (Fig. 1D). Phospho-flow cytometric analysis of Lin⁻/cKit⁺/CD105⁻/CD34⁺ bone marrow cells, which are highly enriched for myeloid progenitors (Supplementary Fig. S2C), revealed elevated basal levels of phosphorylated extracellular signal-regulated kinase (pERK) and enhanced responsiveness to GM-CSF in *Nras*^{G12D/G12D} cells compared with heterozygous and hemizygous *Nras*^{G12D}-mutant cells (Fig. 1E). In summary, phenotypic, functional, and biochemical analyses of age and strain-matched mice indicate that WT *Nras* lacks tumor suppressor activity in the hematopoietic lineage.

To determine whether exogenous WT *Nras* expression might antagonize the abnormal growth of *Nras*^{G12D/G12D} cells, we infected *Mx1-Cre;Nras*^{G12D/G12D} bone marrow with murine stem cell virus (MSCV) vectors encoding N-terminal GFP fused to WT N-Ras (N-Ras^{WT}), WT K-Ras (K-Ras^{WT}), or dominant negative N-Ras (N-Ras^{N17}; ref. 9). After sorting to isolate GFP-positive (GFP⁺) cells, CFU-GM colony growth was assayed in the presence of GM-CSF. *Mx1-Cre;Nras*^{G12D/G12D} bone marrow formed significantly more CFU-GM colonies than heterozygous or hemizygous *Nras* cells (Fig. 2A). Expressing N-Ras^{WT} or K-Ras^{WT} had no effect on CFU-GM colony growth from *Nras*^{G12D/G12D} bone marrow, whereas dominant negative N-Ras^{N17} reduced growth by more than twofold (Fig. 2A).

To further investigate whether WT N-Ras interferes with oncogenic N-Ras^{G12D}-induced myeloid transformation, we infected WT fetal liver cells with MSCV vectors expressing N-terminal mCherry-tagged N-Ras^{G12D} in combination with GFP, GFP-tagged N-Ras^{WT}, or GFP-tagged K-Ras^{WT}. Flow cytometry and Western blotting revealed an equivalent increase in Ras protein levels in cotransduced cells (Fig. 2B and C). Importantly, neither WT Ras isoform suppressed the aberrant pattern of cytokine-independent CFU-GM progenitor growth induced by exogenous N-Ras^{G12D} expression (Fig. 2D).

We next assessed the functional and biochemical consequences of varying *Nras* oncogene dosage by infecting WT fetal hematopoietic cells with viruses encoding GFP-tagged N-Ras^{G12D} and sorting for different levels of GFP expression (Fig. 3A). As expected, increasing GFP intensity correlated with higher N-Ras protein levels (Fig. 3B). Progenitors expressing the highest levels of N-Ras^{G12D} showed cytokine-independent CFU-GM colony growth with a threshold level of expression required for myeloid transformation (Fig. 3B and C).

We also interrogated Ras signaling in transduced GFP⁺ bone marrow-derived macrophages that were first deprived of cytokines and serum and then stimulated with GM-CSF (10).

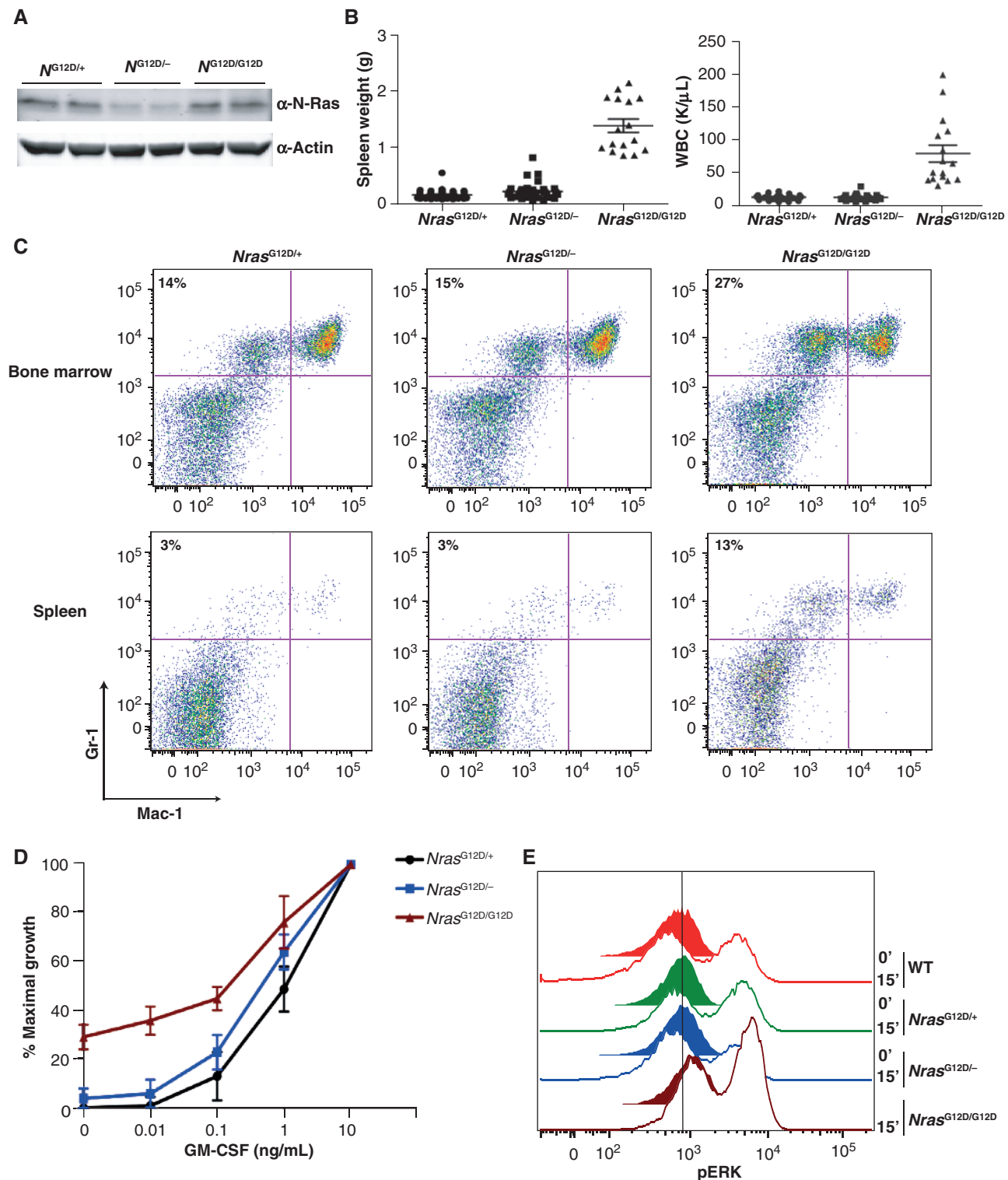


Figure 1. Dominant effects of *Nras*^{G12D} dosage in hematologic disease. **A**, Western blot analysis of bone marrow lysates from 6-week-old mice shows reduced total N-Ras protein levels in hemizygous *Nras*^{G12D} mice. **B**, spleen weights and white blood cell (WBC) counts of 6-month-old heterozygous ($n = 38$), hemizygous ($n = 32$), and homozygous ($n = 20$) *Nras*^{G12D} mice. **C**, representative flow cytometric analysis of bone marrow and spleen specimens from all three genotypes with the myeloid markers Gr-1 and Mac-1. The percentage of immature monocytic (Gr-1^{lo}, Mac-1^{hi}) cells is shown on each panel. **D**, CFU-GM colony growth from *Nras*^{G12D/+} (black line), *Nras*^{G12D/−} (blue line), and *Nras*^{G12D/G12D} (red line) bone marrow cells over a range of GM-CSF concentrations ($n = 5$ – 7 per genotype). Note that only *Nras*^{G12D/G12D} cells show cytokine-independent progenitor growth. **E**, flow cytometric analysis of basal ERK phosphorylation in Lin[−] c-Kit⁺ CD105[−] CD34⁺ bone marrow cells from 3-month-old mice and response to GM-CSF stimulation (10 ng/mL for 15 minutes). The vertical black line indicates basal pERK levels in WT cells.

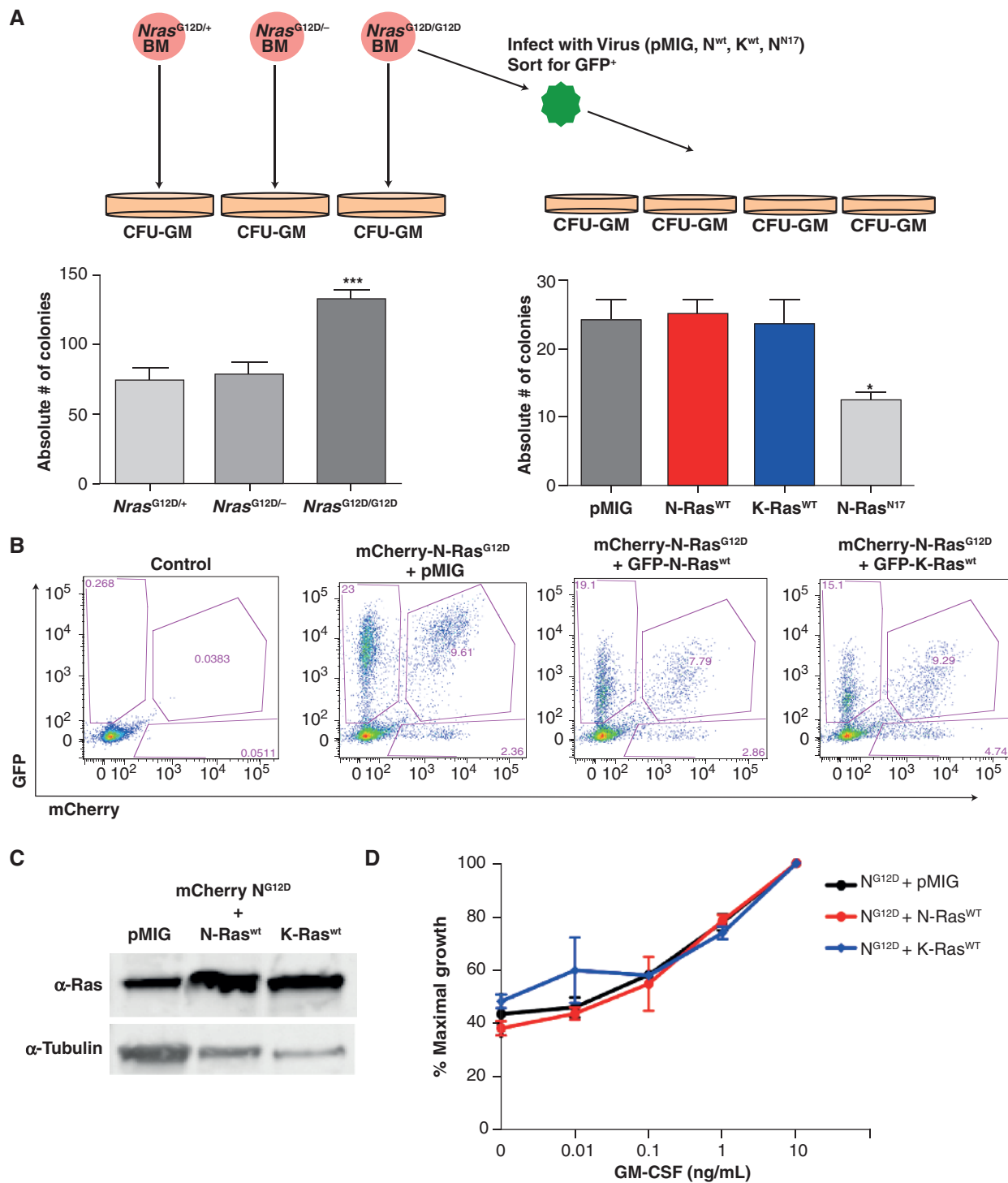


Figure 2. Wild-type Ras does not antagonize myeloid transformation by *Nras*^{G12D}. **A**, CFU-GM progenitor growth from *Nras*^{G12D/+}, *Nras*^{G12D/-}, and *Nras*^{G12D/G12D} ($n = 6$ from each genotype) bone marrow (BM) cells in the presence of 1 ng/mL GM-CSF ($***P < 0.0001$; left). Bone marrow from *Nras*^{G12D/G12D} mice was infected with MSCVs encoding GFP-tagged WT N-Ras (N-Ras^{WT}), WT K-Ras (K-Ras^{WT}), or a dominant negative N-Ras protein (N-Ras^{N17}; right). After sorting to isolative GFP⁺ cells, CFU-GM colonies were grown in the presence of 1 ng/mL GM-CSF. The data presented are from three independent experiments (*, $P = 0.0135$). **B**, WT E14.5 fetal liver cells were cotransduced with MSCVs expressing mCherry-N-Ras^{G12D} and either GFP-only (pMIG), GFP-N-Ras^{WT}, or GFP-K-Ras^{WT}. Flow cytometric analyses indicate equivalent numbers of PE-Texas Red (mCherry) and FITC (GFP) double-positive cells. The GFP fluorescence is higher in cells expressing GFP only. **C**, Immunoblot analysis shows that cells cotransduced with oncogenic N-Ras^{G12D} and WT N-Ras or WT K-Ras express more total Ras than control cells transduced with N-Ras^{G12D} and an "empty" MIG vector. **D**, CFU-GM colony growth from sorted cells expressing both GFP and mCherry over a range of GM-CSF concentrations. N-Ras^{G12D} transforms approximately 40% of myeloid progenitors to cytokine-independent growth, and coexpressing WT N-Ras or K-Ras does not alter this phenotype.

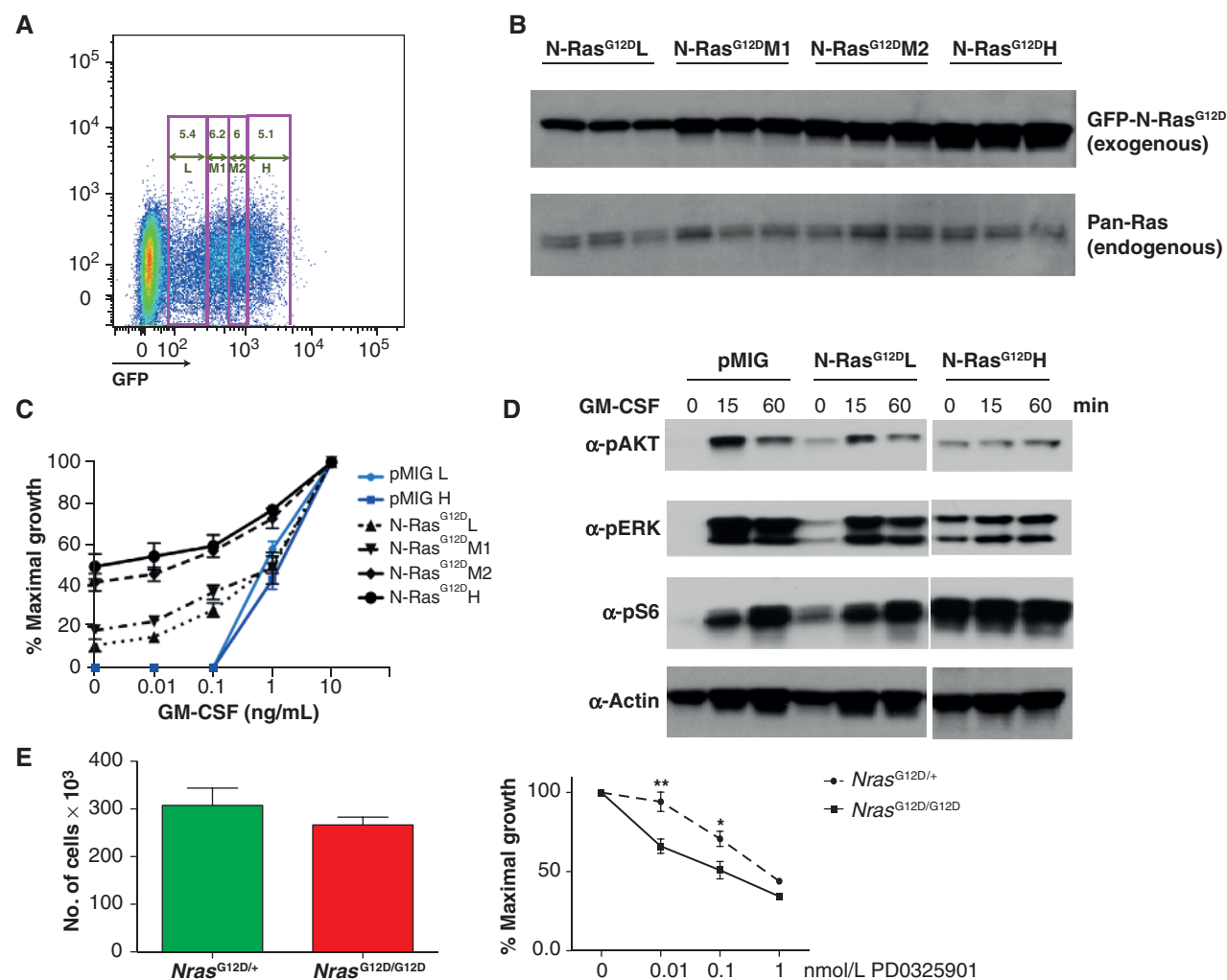


Figure 3. Oncogenic *NRAS*^{G12D} signaling is dosage dependent. **A**, subpopulations of WT E14.5 fetal liver cells were infected with a virus expressing GFP-N-Ras^{G12D} and isolated by sorting based on the level of GFP fluorescence (L-low, M1-low medium, M2-high medium, H-high). **B**, immunoblot analysis of macrophages grown from fetal liver cells in **A** indicates that N-Ras levels correlate with GFP positivity. **C**, CFU-GM colony growth from fetal liver cells expressing L, M1, M2, and H levels of GFP-N-Ras^{G12D}. **D**, the macrophages shown in **B** were starved overnight and then stimulated with 10 ng/mL of GM-CSF for 15 or 60 minutes. Levels of phosphorylated ERK, AKT, and S6 were assessed by Western blotting. **E**, growth of cultured bone marrow-derived macrophages from 26-week-old *Mx1-Cre;Nras^{G12D/G12D}* (n = 4) and *Mx1-Cre;Nras^{G12D/+}* (n = 5) mice. Total cell numbers after 5 days in the absence of PD0325901 (left). Percentage reduction in cell numbers in cells exposed to 0.01, 0.1, and 1 nmol/L of PD0325901 for 5 days (right). Asterisks denote significant differences between *Nras^{G12D/G12D}* and *Mx1-Cre;Nras^{G12D/+}* (*, *P* = 0.0425; **, *P* = 0.0076).

Under these conditions, AKT, ERK, and S6 were not phosphorylated in starved macrophages infected with the empty pMIG vector, and these cells responded robustly to GM-CSF stimulation (Fig. 3D). Macrophages expressing low levels of N-Ras^{G12D} showed a modest increase in basal pAKT, pERK, and pS6, which were augmented by cytokine stimulation. In contrast, starved cells expressing the highest levels of N-Ras^{G12D} exhibited a further increase in basal levels of all three phospho proteins, but were unresponsive to GM-CSF (Fig. 3D). Thus, Akt and Erk activation are uncoupled from cytokine stimulation in primary myeloid cells expressing high levels of oncogenic N-Ras.

Treatment with the potent and selective MAP-ERK kinase (MEK) inhibitor PD0325901 restores a normal pattern of hematopoiesis in *Kras*- and *Nf1*-mutant mice with myeloproliferative neoplasm (11, 12). We therefore asked whether endog-

enous *Nras*^{G12D} gene dosage influences the sensitivity of bone marrow-derived macrophages to MEK inhibition. Macrophages grown directly from the bone marrows of *Mx1-Cre;Nras^{G12D/+}* and *Mx1-Cre;Nras^{G12D/G12D}* mice expanded to a similar extent in the presence of a saturating concentration macrophage colony-stimulating factor (M-CSF; Fig. 3E). Remarkably, low concentrations of PD0325901 selectively reduced the growth of homozygous *Nras*-mutant macrophages (Fig. 3E) despite similar basal levels of ERK activation and sensitivity to inhibition by MEK inhibitor treatment (Supplementary Fig. S3A and S3B).

Nras^{G12D} expression cooperated with the MOL4070LTR retrovirus to efficiently induce AML in *Mx1-Cre;Nras^{G12D/+}* mice that recapitulates morphologic and genetic features of human *Nras*-mutant AMLs (4). Somatic loss of the WT *Nras* allele occurs in many of these leukemias (Supplementary

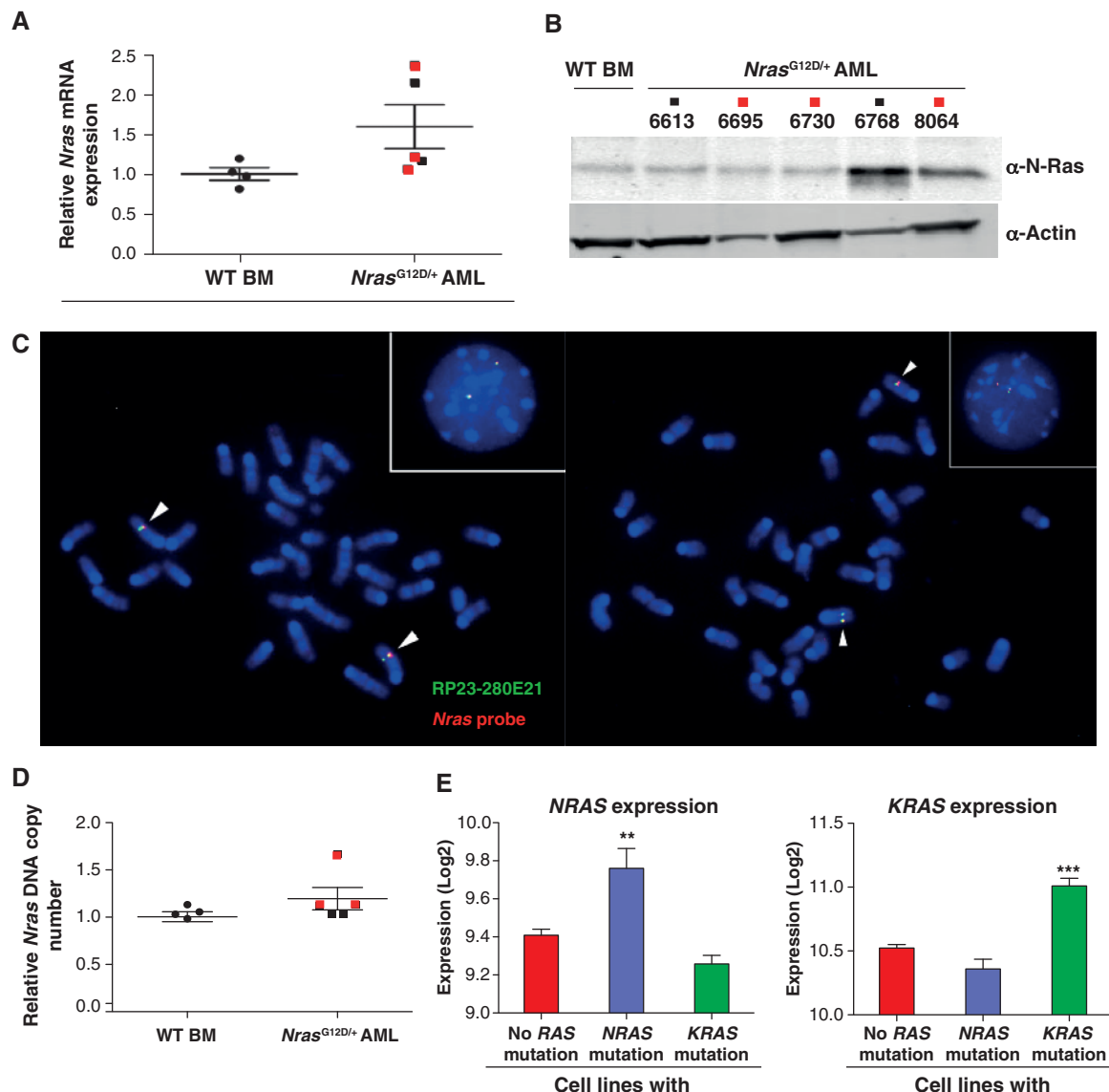


Figure 4. N-Ras expression in AMLs from *Nras*^{G12D/+} mice. **A**, quantitative real-time PCR of *Nras* mRNA expression in WT bone marrow (BM) and primary *Nras*^{G12D} AMLs with and without loss of constitutional heterozygosity (LOH) (*Nras*^{G12D} leukemias with loss of or a marked reduction in the WT allele are shown in red and AMLs that retain the WT allele are in black). **B**, Western blot analysis of *Nras*^{G12D} AMLs shows that N-Ras protein levels are equivalent to or higher than in WT mouse bone marrow. **C**, FISH analysis of metaphase and interphase cells from representative AMLs with (#6730; left) and without (#6768; right) LOH. Arrowheads identify a fused signal from both BAC probe RP23-280E21 and the smaller *Nras* probe. Hybridizing with the larger BAC clone uniformly revealed signals on both chromosomal homologs in all 5 *Nras*^{G12D} AMLs. Equal percentages of cells showed one or two hybridization signals (shown here) with the much smaller *Nras*-specific probe from AMLs with and without LOH. **D**, *Nras* DNA copy number is normal or increased in *Nras*^{G12D} AMLs with and without LOH as assessed by TaqMan quantitative PCR. **E**, *NRAS* and *KRAS* expression in 957 human cancer cell lines with *NRAS* mutations ($n = 56$), *KRAS* mutations ($n = 173$), or no *RAS* mutation ($n = 728$). **, $P = 0.0018$; ***, $P = 7.7 \times 10^{-16}$. BAC, bacterial artificial chromosome.

Fig. S4A; ref. 4). Importantly, however, real-time quantitative PCR analysis showed that *Nras* expression is normal or increased in AML blasts (Fig. 4A). Interestingly, *Kras* expression was reduced to levels below that in WT bone marrow (Supplementary Fig. S4B). Consistent with these data, Western blot analysis revealed elevated N-Ras protein levels in AML blasts, including *Nras*^{G12D} leukemias with somatic loss of the normal *Nras* allele (Fig. 4B). We conducted FISH to investigate the mechanism underlying somatic *Nras* inactivation in leukemias with loss of constitutional heterozygosity (LOH)

and also used TaqMan PCR to assess *Nras* copy number. Both analyses supported somatic uniparental disomy (UPD) with duplication of the oncogenic *Nras*^{G12D} allele as the genetic basis underlying loss of the WT *Nras* allele in leukemias with LOH (Fig. 4C and D). Together, these studies indicate that genetic and transcriptional mechanisms converge to augment oncogenic N-Ras^{G12D} expression in AML.

To address the broad relevance of increased *RAS* oncogene expression in human cancer, we queried *NRAS*/*KRAS* mutational status and corresponding expression data across 957

cancer cell lines from different tissues (13). Cancer cell lines with *NRAS* mutations showed a highly significant increase in *NRAS* expression (Fig. 4E). Similarly, lines with *KRAS* mutations expressed more *KRAS* transcript on average. Furthermore, cancer cell lines with *NRAS* mutations showed a significant reduction in *KRAS* expression, whereas those with *KRAS* mutations downregulated *NRAS* (Fig. 4E). Similar trends were observed when the hematopoietic cell lines in this large collection were analyzed separately (Supplementary Fig. S5A). Gene expression data from a well-annotated collection of human AMLs revealed elevated *NRAS* expression compared with normal CD34⁺ progenitors in leukemias with and without *Nras* mutations (Supplementary Fig. S5B).

DISCUSSION

LOH is common in human cancer and classically represents a genetic “second hit” that results in homozygous inactivation of tumor suppressor genes (TSG) that negatively regulate cell growth through diverse mechanisms. Given this, the finding of frequent somatic oncogenic *Ras* mutations and loss of the corresponding WT allele in mouse cancers induced by chemical carcinogenesis raised the possibility that normal *Ras* proteins might also restrain malignant growth (2). Indeed, subsequent experiments showing that germline inactivation of one *Ras* allele greatly increased the incidence and biologic aggressiveness of genotoxin-induced skin and lung carcinoma supported this idea (5, 14). Though provocative, it has proven difficult to reconcile these genetic data with the dominant transforming ability of oncogenic *Ras* proteins and their biochemical properties. Although normal *Ras* genes may function to suppress tumorigenesis in some cell lineages, loss of the normal *Ras* allele may reflect selective pressure for cancers to increase oncogene dosage as they evolve. This idea is compatible with data showing that spontaneous transformation in primary *Hras*-mutant fibroblasts is associated with amplification of the mutant allele (15) and with frequent copy number gains, mutant allele-specific imbalance, and overexpression of oncogenic *KRAS* in human cancer cell lines (16). Interestingly, oncogenic *Hras* amplification is an early event in murine skin carcinogenesis models and may be associated with somatic UPD (2, 17).

Somatic *NRAS* mutations are common in hematologic malignancies, and *Mx1-Cre;Nras*^{G12D} mice provide a tractable and genetically accurate system for interrogating the putative TSG activity of WT *Nras* in early (myeloproliferative neoplasm) and late (AML) stage cancers that do not rely on chemical carcinogenesis. Our extensive genetic and functional analysis indicates that WT *Nras* lacks tumor suppressor activity *in vitro* and *in vivo*, and identifies increased oncogene expression as the major “driver” of aberrant growth. Consistent with these data, oncogenic *NRAS* mutations with UPD have been reported in human AML (18). A JMML with an *NRAS* mutation that acquired UPD after evolution to AML suggests a role of increased oncogenic *NRAS* dosage in disease progression (19). The pattern of *Ras* gene expression in murine *Nras*-mutant leukemias and in human cancer cell lines with oncogenic *RAS* mutations also supports the existence of selective pressure to amplify oncogenic signaling by

increasing oncoprotein levels while simultaneously down-regulating normal *Ras*.

The dominant role of mutant *Ras* amplification is consistent with data showing that expressing oncogenic K-Ras^{G12D} and N-Ras^{G12D} from their endogenous genetic loci results in remarkably little activation of canonical effectors in primary cells, which likely reflects the inhibitory effects of potent cellular feedback responses (20, 21). The dramatic effects of modulating N-Ras^{G12D} protein levels on basal activation of *Ras* effectors and on cytokine responses further suggest that cancer cells must titrate an “optimal” level of pathway activation to overcome negative feedback inhibition without evoking cell-cycle arrest or senescence.

The idea that normal *Ras* proteins might antagonize the transforming properties of their oncogenic counterparts suggested potential therapeutic strategies. Although this possibility remains viable in tissues such as skin and lung where normal *RAS* genes are likely to function as tumor suppressors, our data strongly argue that restoring or enhancing normal *Ras* expression will be ineffective in leukemias with oncogenic *NRAS* mutations. They also support revisiting this general question in other cancers, particularly given the broad pattern of elevated *NRAS* or *KRAS* expression in human cancer cell lines with mutations in each gene. Furthermore, as cancer cells amplify oncogenic signaling to optimize growth, they may become more dependent upon (“addicted to”) these activated pathways, which might be exploited therapeutically. The enhanced dependence of *Nras*^{G12D/G12D} macrophages on MEK supports this idea. Similarly, somatic UPD is common in AML with oncogenic *FLT3* mutations and is associated with resistance to conventional anticancer agents (22). However, these leukemias are more sensitive to *FLT3* inhibitors than AMLs without UPD (23). Thus, selective pressure favoring the outgrowth of clones with increased oncogenic *RAS* gene expression may also render them more susceptible to inhibitors of critical effector pathways.

METHODS

Mouse Strains and Pathologic Analysis

Nras^{2lox2} mice were generated by inserting loxP sites onto each side of exon 2 of the endogenous *Nras* locus in V26.2 C57BL/6 embryonic stem cells (24). A Frt-flanked *Neo* resistance cassette was also inserted into intron 1 (Supplementary Fig. S1A). After germline transmission of the targeted allele, the *Neo* resistance cassette was removed by crossing to an Flp deleter strain (Jackson Laboratory). *Mx1-Cre;Nras*^{G12D} mice were intercrossed with *Nras*^{2lox2} mice to generate *Mx1-Cre;Nras*^{G12D/G12D}, *Mx1-Cre;Nras*^{G12D/+}, and *Mx1-Cre;Nras*^{G12D/2lox2} mice. All mice received a single intraperitoneal injection of poly-I/poly-C (250 µg) at 3 weeks of age to activate *Mx1-Cre* expression (4). Mice were euthanized at 6 months of age to assess disease. Pathologic examinations were conducted as previously described (4).

Hematopoietic Progenitor Assays and Flow Cytometry

Hematopoietic progenitor assays and flow cytometric analyses were conducted as previously described (4, 10).

Retroviral Transduction

Nras^{WT}, *Kras*^{WT}, *Nras*^{N17}, and *Nras*^{G12D} alleles containing either N-terminal GFP or N-terminal mCherry markers were cloned into the MSCV with expression driven by the internal ribosomal entry

RESEARCH BRIEF

Xu et al.

site. Retrovirally transduced E14.5 fetal liver cells from C57Bl/6 mice were sorted to isolate GFP⁺ cells, which were plated in methylcellulose medium to assess CFU-GM growth as described previously (4).

Biochemistry

Biochemical analyses were conducted on cultured macrophages that were differentiated from transduced GFP⁺ fetal liver cells in 50 ng/mL M-CSF as described previously (10). Quantitative effects of PD0325901 on macrophage ERK signaling were determined by imaging and quantifying blots on an Odyssey imager.

FISH Analysis

A labeled BAC probe containing the mouse *Nras* gene (RP23-280E21; 150 kb) was labeled with 5-(3-aminoallyl)-dUTP by nick translation, followed by chemical labeling with amine-reactive Alexa Fluor 488 using the Ares DNA labeling kit. An 8-kb genomic probe containing the *Nras* gene was labeled with biotin-dUTP by nick translation and detected with streptavidin conjugated with Alexa Fluor 568. FISH was conducted as described previously (25). Cells were counterstained with 4, 6 diamidino-2-phenylindole-dihydrochloride. A minimum of 200 interphase nuclei and 10 metaphase cells were scored for each sample.

RNA Purification and Quantitative PCR Analysis

RNA purification and quantitative PCR analyses of primary AML cells that were generated by infecting *Nras*^{G12D/+} mice with the MOL4070LTR retrovirus were conducted as previously described (4).

TaqMan PCR

Genomic DNA from *Nras*-mutant AMLs was purified using a Qia-gen RNEasy Mini kit. A total of 10 ng of DNA was used as a template for quantitative PCR experiments. The sequence for murine transferin receptor (*mTfrc*) was used to normalize total amounts of DNA. The premixed probe and primer assay mixture used to quantify total amounts of genomic *Nras* were purchased from Applied Biosystems.

Macrophage Proliferation Assay

A total of 8×10^5 bone marrow-derived macrophages from *Mx1-Cre;Nras*^{G12D/G12D} or *Mx1-Cre;Nras*^{G12D/+} mice were plated in triplicate in 12-well plates in the presence of 10 ng/mL M-CSF and varying doses of PD0325901. Total numbers of viable cells were counted using the Beckman Coulter Vi-Cell XR at day 5.

Gene Expression Profiling of Cell Line and AML

NRAS and *KRAS* expression in cancer cell lines was extracted from gene-centric RMA-normalized mRNA expression data downloaded from Cancer Cell Line Encyclopedia (13). *KRAS* and *NRAS* mutational status was determined by hybrid capture and OncoPrint assays. *P* values were calculated by two-tailed Student *t* test assuming unequal variance. To further examine *NRAS* and *KRAS* expression in human leukemia, we conducted microarray-based gene expression profiling data of pediatric AML and normal CD34⁺ samples generated using Affymetrix U133A microarrays (Affymetrix) according to the manufacturer's instructions, with data processed using MAS5 normalization and log₂ transformation (26). This cohort comprised 108 samples including CD34⁺ bone marrow cells (*n* = 4), and included 74 without an *NRAS* mutation and 30 with a mutation. Primary data are available through <http://www.ncbi.nlm.nih.gov/geo/> accession numbers GSE43176 (AML samples) and GSE33315 (CD34⁺ bone marrow).

No experiments were carried out on any cell lines to generate these data. All mouse experiments were approved by the Institutional Animal Care and Use Committee of the University of California, San Francisco.

Disclosure of Potential Conflicts of Interest

No potential conflicts of interest were disclosed.

Authors' Contributions

Conception and design: J. Xu, K. Shannon

Development of methodology: J. Xu, T. Jacks

Acquisition of data (provided animals, acquired and managed patients, provided facilities, etc.): J. Xu, K.M. Haigis, A.J. Firestone, Q. Li, J. Downing, M.M. Le Beau

Analysis and interpretation of data (e.g., statistical analysis, biostatistics, computational analysis): J. Xu, A.J. Firestone, M.E. McEnerney, Q. Li, S.-C. Chen, J. Nakitandwe, J. Downing, M.M. Le Beau, K. Shannon

Writing, review, and/or revision of the manuscript: J. Xu, J. Nakitandwe, J. Downing, M.M. Le Beau, K. Shannon

Study supervision: M.M. Le Beau, K. Shannon

Performed the FISH analysis of the samples: E. Davis

Acknowledgments

The authors thank J. Leopold (Pfizer, Inc.) for PD0325901 and A. Balmain and F. McCormick for suggestions. The authors also thank T. Huang and E. Hwang for assistance in critical experiments.

Grant Support

This work was supported by NIH grants R37CA72614, P01CA40046, and K08CA134649, a Specialized Center of Research award from the Leukemia and Lymphoma Society (LLS 7019-04), the American Lebanese Syrian Associated Charities (ALSAC) of St. Jude Children's Research Hospital, an American Cancer Society Fellowship (to J. Xu), and a Damon Runyon Cancer Research Foundation Fellowship (DRG-2149-13; to A.J. Firestone).

Received March 5, 2013; revised May 23, 2013; accepted May 28, 2013; published OnlineFirst June 3, 2013.

REFERENCES

- Schubbert S, Shannon K, Bollag G. Hyperactive Ras in developmental disorders and cancer. *Nat Rev Cancer* 2007;7:295–308.
- Bremner R, Balmain A. Genetic changes in skin tumor progression: correlation between presence of a mutant ras gene and loss of heterozygosity on mouse chromosome 7. *Cell* 1990;61:407–17.
- To MD, Wong CE, Karnezis AN, Del Rosario R, Di Lauro R, Balmain A. Kras regulatory elements and exon 4A determine mutation specificity in lung cancer. *Nat Genet* 2008;40:1240–4.
- Li Q, Haigis KM, McDaniel A, Harding-Theobald E, Kogan SC, Akagi K, et al. Hematopoiesis and leukemogenesis in mice expressing oncogenic *Nras*^{G12D} from the endogenous locus. *Blood* 2011;117:2022–32.
- Zhang Z, Wang Y, Vikis HG, Johnson L, Liu G, Li J, et al. Wildtype *Kras*² can inhibit lung carcinogenesis in mice. *Nat Genet* 2001;29:25–33.
- Wang J, Liu Y, Li Z, Du J, Ryu MJ, Taylor PR, et al. Endogenous oncogenic *Nras* mutation promotes aberrant GM-CSF signaling in granulocytic/monocytic precursors in a murine model of chronic myelomonocytic leukemia. *Blood* 2010;116:5991–6002.
- Ward AF, Braun BS, Shannon KM. Targeting oncogenic Ras signaling in hematologic malignancies. *Blood* 2012;120:3397–406.
- Wang J, Liu Y, Li Z, Wang Z, Tan LX, Ryu MJ, et al. Endogenous oncogenic *Nras* mutation initiates hematopoietic malignancies in a dose- and cell type-dependent manner. *Blood* 2011;118:368–79.
- Xu J, Hedberg C, Dekker FJ, Li Q, Haigis KM, Hwang E, et al. Inhibiting the palmitoylation/depalmitoylation cycle selectively reduces the growth of hematopoietic cells expressing oncogenic *Nras*. *Blood* 2012;119:1032–5.
- Schubbert S, Zenker M, Rowe SL, Böll S, Klein C, Bollag G, et al. Germline *KRAS* mutations cause Noonan syndrome. *Nat Genet* 2006;38:331–6.

11. Chang T, Krisman K, Theobald EH, Xu J, Akutagawa J, Lauchle JO, et al. Sustained MEK inhibition abrogates myeloproliferative disease in *Nf1* mutant mice. *J Clin Invest* 2013;123:335–9.
12. Lyubynska N, Gorman MF, Lauchle JO, Hong WX, Akutagawa JK, Shannon K, et al. A MEK inhibitor abrogates myeloproliferative disease in *Kras* mutant mice. *Sci Transl Med* 2011;3:76ra27.
13. Barretina J, Caponigro G, Stransky N, Venkatesan K, Margolin AA, Kim S, et al. The cancer cell line encyclopedia enables predictive modelling of anticancer drug sensitivity. *Nature* 2012;483:603–7.
14. To MD, Rosario RD, Westcott PM, Banta KL, Balmain A. Interactions between wild-type and mutant *Ras* genes in lung and skin carcinogenesis. *Oncogene* 2012 Sep 3. [Epub ahead of print].
15. Finney RE, Bishop JM. Predisposition to neoplastic transformation caused by gene replacement of *H-ras1*. *Science* 1993;260:1524–7.
16. Soh J, Okumura N, Lockwood WW, Yamamoto H, Shigematsu H, Zhang W, et al. Oncogene mutations, copy number gains and mutant allele specific imbalance (MASI) frequently occur together in tumor cells. *PLoS ONE* 2009;4:e7464.
17. Chen X, Mitsutake N, LaPerle K, Akeno N, Zanzonico P, Longo VA, et al. Endogenous expression of *Hras*(G12V) induces developmental defects and neoplasms with copy number imbalances of the oncogene. *Proc Natl Acad Sci U S A* 2009;106:7979–84.
18. Dunbar AJ, Gondek LP, O'Keefe CL, Makishima H, Rataul MS, Szpurka H, et al. 250K single nucleotide polymorphism array karyotyping identifies acquired uniparental disomy and homozygous mutations, including novel missense substitutions of *c-Cbl*, in myeloid malignancies. *Cancer Res* 2008;68:10349–57.
19. Matsuda K, Nakazawa Y, Sakashita K, Shiohara M, Yamauchi K, Koike K. Acquisition of loss of the wild-type *NRAS* locus with aggressive disease progression in a patient with juvenile myelomonocytic leukemia and a heterozygous *NRAS* mutation. *Haematologica* 2007;92:1576–8.
20. Tuveson DA, Shaw AT, Willis NA, Silver DP, Jackson EL, Chang S, et al. Endogenous oncogenic *K-ras*(G12D) stimulates proliferation and widespread neoplastic and developmental defects. *Cancer Cell* 2004;5:375–87.
21. Chandarlapaty S, Sawai A, Scaltriti M, Rodrik-Outmezguine V, Grbovic-Huezo O, Serra V, et al. AKT inhibition relieves feedback suppression of receptor tyrosine kinase expression and activity. *Cancer Cell* 2011;19:58–71.
22. Pratz KW, Sato T, Murphy KM, Stine A, Rajkhowa T, Levis M. FLT3-mutant allelic burden and clinical status are predictive of response to FLT3 inhibitors in AML. *Blood* 2010;115:1425–32.
23. Gale RE, Green C, Allen C, Mead AJ, Burnett AK, Hills RK, et al. The impact of FLT3 internal tandem duplication mutant level, number, size, and interaction with *NPM1* mutations in a large cohort of young adult patients with acute myeloid leukemia. *Blood* 2008;111:2776–84.
24. Haigis KM, Kendall KR, Wang Y, Cheung A, Haigis MC, Glickman JN, et al. Differential effects of oncogenic *K-Ras* and *N-Ras* on proliferation, differentiation and tumor progression in the colon. *Nat Genet* 2008;40:600–8.
25. Le Beau MM, Espinosa R, Davis EM, Eisenbart JD, Larson RA, Green ED. Cytogenetic and molecular delineation of a region of chromosome 7 commonly deleted in malignant myeloid diseases. *Blood* 1996;88:1930–5.
26. Zhang J, Ding L, Holmfeldt L, Wu G, Heatley SL, Payne-Turner D, et al. The genetic basis of early T-cell precursor acute lymphoblastic leukaemia. *Nature* 2012;481:157–63.

CANCER DISCOVERY

Dominant Role of Oncogene Dosage and Absence of Tumor Suppressor Activity in *Nras*-Driven Hematopoietic Transformation

Jin Xu, Kevin M. Haigis, Ari J. Firestone, et al.

Cancer Discovery 2013;3:993-1001. Published OnlineFirst June 3, 2013.

Updated version	Access the most recent version of this article at: doi: 10.1158/2159-8290.CD-13-0096
Supplementary Material	Access the most recent supplemental material at: http://cancerdiscovery.aacrjournals.org/content/suppl/2013/05/31/2159-8290.CD-13-0096.DC1

Cited articles	This article cites 25 articles, 13 of which you can access for free at: http://cancerdiscovery.aacrjournals.org/content/3/9/993.full#ref-list-1
Citing articles	This article has been cited by 9 HighWire-hosted articles. Access the articles at: http://cancerdiscovery.aacrjournals.org/content/3/9/993.full#related-urls

E-mail alerts	Sign up to receive free email-alerts related to this article or journal.
Reprints and Subscriptions	To order reprints of this article or to subscribe to the journal, contact the AACR Publications Department at pubs@aacr.org .
Permissions	To request permission to re-use all or part of this article, use this link http://cancerdiscovery.aacrjournals.org/content/3/9/993 . Click on "Request Permissions" which will take you to the Copyright Clearance Center's (CCC) Rightslink site.